Pattern formation in drying water films

N. Samid-Merzel, S. G. Lipson, and D. S. Tannhauser
Department of Physics, Technion–Israel Institute of Technology, 32000 Haifa, Israel
(Received 19 September 1997)

A film of a volatile medium in contact with unsaturated vapor is bound to a plane substrate by both van der Waals and polar forces. We present a thermodynamic description of this system, including exchange of material between the fluid and the vapor under nonequilibrium conditions. For a range of values of the vapor pressure, a two-phase system develops, involving the coexistence of molecularly thin and macroscopically thick layers whose dynamics are controlled by the vapor pressure. The theory is used to explain the origin of experimentally observed spatial patterns in water films evaporating from clean mica substrates, where scale and other features are a function of the vapor pressure. An analogy is developed between the initial stages of the pattern formation and the diffusion-controlled solidification problem in two dimensions and typical features such as ''doublons'' or parity-broken dendrites are observed. At later stages in the pattern formation hydrodynamics becomes important. [S1063-651X(98)05003-X]

PACS number(s): 47.54.+r, 68.45.Gd, 68.70.+w

I. INTRODUCTION

In recent years there has been a growing interest in the dynamics of spontaneous pattern formation in simple systems [1,2]. A particular challenge in this field is to find experimental systems that are sufficiently simple and well understood to allow a quantitative theoretical analysis that enables a direct comparison between the patterns observed in experiments and those predicted by theory. One limiting factor is that much theoretical work and particularly numerical calculations have been limited to two-dimensional systems. Recently [3,4] we have been studying the patterns that form when initially thick water films are allowed to evaporate from mica substrates under varying degrees of subsaturation. In trying to understand the physics underlying this process we have come to the conclusion that they represent a particularly simple example of a two-dimensional isotropic nonlinear system that can easily be compared with theoretical work and computer simulations. Indeed, one of the features that led us in this direction was a remarkable similarity between some of the patterns observed and those appearing in simulations of diffusion-controlled growth of a two-dimensional solid from a supercooled melt [5,6]. These features have been called ''doublons'' or parity-broken dendrites.

In this paper we present a thermodynamic description of the dewetting process that can occur when a volatile film evaporates from a substrate to which it is bound by both van der Waals and polar forces and show that the initial stages of the pattern formation can be described in a manner analogous to the diffusion-controlled solidification problem in two dimensions. Later stages of the pattern formation are controlled by hydrodynamics and constitute a different type of problem [7]. Although most of this paper is concerned with the thermodynamics of the process, reference will be made to some of the experimental results in order to demonstrate quantitative relevance. The experimental results will be described fully elsewhere [8].

Wetting and nonwetting films on a substrate

The statics and dynamics of a thin film on a substrate have been discussed extensively by Sharma and Jameel [9–11], de Gennes [12] and Israelachvili [13] and experiments on similar systems have been reported by Reiter [14] and Brochard-Wyart and co-workers [15]. However, these works are limited to nonvolatile films, within which mass is conserved. In the situation that is the subject of this paper the film is in contact with vapor and the transfer of mass between the two has to be taken into account.

When a uniform layer of a fluid on a substrate evaporates, several scenarios are possible. The first takes place when the fluid *does not wet* the substrate. In this case a large enough quantity of fluid on a fixed area of substrate will form a uniform pool because of gravity. When this pool evaporates, at some critical thickness an instability occurs and the film breaks up into drops with dry substrate between them. A second scenario occurs if the film *wets* the substrate. Then the layer formed under the same circumstances will remain continuous with uniform thickness that decreases monotonically until the film has completely evaporated.

In a third scenario, which is the subject of the present paper, a layer of water with nonzero thickness remains on the substrate at all times, but for some range of mean thickness a uniform layer is unstable and the film breaks up into a two-phase system. Then evaporation of the film is a more complicated process and pattern formation may occur.

The experiments carried out by Reiter [14] and Brochard-Wyart and co-workers [15] correspond to the first scenario, although in these cases the instability was not induced by thinning through evaporation. In the second case of wetting films, the thickness of equilibrium films of various fluids on substrates has been determined experimentally [16]. The third scenario has been discussed theoretically for a nonvolatile liquid by Sharma and Jameel [9–11], but little experimental investigation has been carried out [14]. To our knowledge, a theory for a volatile fluid has not been reported.

In our experiments [3,4] water is deposited on a cleaved mica substrate from a saturated vapor phase (vapor pressure p_s) at a given temperature. The film is observed optically by interference microscopy. It initially forms a thick wetting layer, typically 1 μm thick or more. If the substrate tempera-

ture is now raised slightly so that the vapor becomes unsaturated with respect to it, the layer starts to evaporate. The layer is observed to thin uniformly until it reaches a few tens of nanometers thickness, at which point an instability occurs, in which very thin circular patches nucleate and spread over the film. Water from a patch accumulates in a rim around its periphery and this rim undergoes an instability as the patch grows, finally producing a complicated pattern of water drops. The scale of the pattern formed during the evaporation is a function of the rate of evaporation and the temperature of the substrate and contains several specific features, which will be discussed elsewhere [8]. It therefore seems that water films go through a region of thicknesses in which uniform wetting is discouraged. Such behavior cannot be explained if the thickness derivative of the interaction potential between the water and the substrate depends monotonically on thickness. (In an earlier paper [17] we claimed to have found an explanation of this phenomenon in the framework of a simple van der Waals type of interaction between the water and the substrate, but this paper has been shown to be incorrect and should be ignored.) Beaglehole and Christenson [16] found experimentally that under subsaturated conditions ($p < 0.97 p_s$) the equilibrium state of water on mica at 18 °C is a very thin (<2 nm) uniform film. The present paper is concerned with the nonequilibrium process by which this state is attained. Similar types of pattern to those observed in water during evaporation have been observed during rupture of nonwetting films [14]. (One should remark that the true equilibrium state for a nonvolatile liquid on a nonwetted substrate is a single drop, but once patterns of isolated drops have formed there is no way, in the absence of either evaporation or an underlying film, by which this equilibrium state can be achieved.)

II. THEORY FOR ZERO VAPOR PRESSURE

In order to establish a common language with earlier work (in particular that of Sharma [9]) we first consider the thermodynamics of a nonvolatile film. The Gibbs free energy of the film is a sum of its bulk energy and surface energy $G = G_1 + G_\sigma$. For a film with zero vapor pressure the volume is constant; since G_1 depends only on the volume and is therefore constant, we can take its value as zero (see also Sec. III A).

A. Equilibrium of a thin film of given length

Even though the film is two dimensional it will be clearer at first to regard it as being one dimensional, i.e., of unit width with properties independent of y. Quantities are defined per unit substrate area unless stated otherwise. The extension to two dimensions, which will be required for discussing pattern formation, is trivial and will be introduced in Sec. III D. The one-dimensional case has already been studied in detail by Sharma and Jameel [10] and Mitlin [18], but we will briefly summarize their work.

A film of length L_0 has height $h(x)$ and volume $\int_0^{L_0} h(x)dx$. The equilibrium shape of the film is found by minimizing the free energy G_σ. We assume for the moment that the film is thick; then

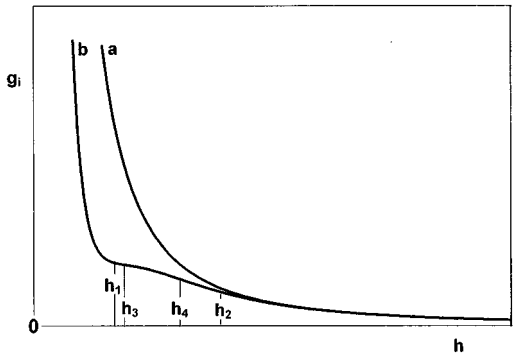

FIG. 1. Interfacial Gibbs free energy g_i, as a function of film thickness h, for the van der Waals interaction with a negative Hamaker constant without (curve a) and with (curve b) the polar interaction term. The significance of h_1 to h_4 is explained in the text.

$$G_\sigma = (\gamma_{\mathrm{SL}} + \gamma_{\mathrm{LV}} - \gamma_{\mathrm{SV}})L_0 + \int_0^{L_0} \frac{\gamma_{LV}}{2}\left(\frac{\partial h}{\partial x}\right)^2 dx, \qquad (1)$$

where γ_{ij} is the surface energy per unit area between bulk phases i and j (substrate, liquid, and vacuum or inert gas) and the integral term results from the sloping parts of the film that increase its area. We have assumed $|\partial h/\partial x|$ to be small.

If the film is thin an additional energy $g_i(h)$ arises from the finite thickness h of the film; it is an addition to the surface energies in Eq. (1). This $g_i(h)$ represents the interaction per unit area between the interfaces when the distance between them is finite. Clearly, $g_i(h) \to 0$ as $h \to \infty$. When $g_i(h)$ is positive and monotonic (Fig. 1, curve a) the film tends to thicken and we have the classical wetting situation. The general expression for G_σ is therefore

$$G_\sigma = [\gamma_{\mathrm{SL}} + \gamma_{\mathrm{LV}} - \gamma_{\mathrm{SV}}]L_0 + \int_0^{L_0}\left[\frac{\gamma_{\mathrm{LV}}}{2}\left(\frac{\partial h}{\partial x}\right)^2 + g_i(h)\right]dx, \qquad (2)$$

i.e., the surface energy per unit area of the substrate is

$$g_\sigma(h) = \gamma_{\mathrm{SL}} = \gamma_{\mathrm{LV}} - \gamma_{\mathrm{SV}} + \frac{\gamma_{\mathrm{LV}}}{2}\left(\frac{\partial h}{\partial x}\right)^2 + g_i(h). \qquad (3)$$

The first terms of Eqs. (2) and (3) are independent of the shape $h(x)$ so in order to minimize G_σ we have to minimize

$$\int_0^{L_0}\left[\frac{\gamma_{\mathrm{LV}}}{2}\left(\frac{\partial h}{\partial x}\right)^2 + g_i(h) - \lambda h(x)\right]dx = \int_0^{L_0} I\left(x, h, \frac{\partial h}{\partial x}\right)dx, \qquad (4)$$

where

$$I = \frac{\gamma_{\mathrm{LV}}}{2}\left(\frac{\partial h}{\partial x}\right)^2 + g_i(h) - \lambda h(x) \qquad (5)$$

and the term $\lambda h(x)$ comes from the constraint of constant volume. The function $h(x)$ that minimizes G_σ obeys the differential equation

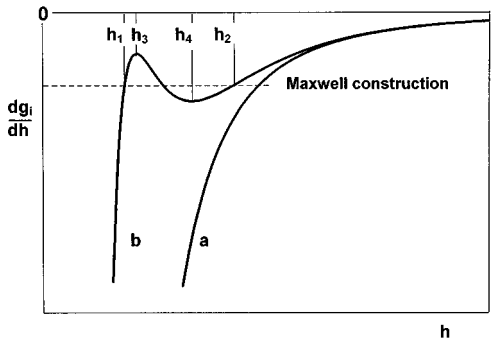

FIG. 2. Same as Fig. 1 showing dg_i/dh.

$$\frac{\partial I}{\partial h}-\frac{\partial}{\partial x}\left(\frac{\partial I}{\partial h_x}\right)=0, \tag{6}$$

giving for a film in equilibrium

$$\frac{dg_i}{dh}-\gamma_{\mathrm{LV}}\frac{\partial^2 h}{\partial x^2}=\lambda. \tag{7}$$

The expression dg_i/dh is the function ϕ defined by Sharma [9]. In Eq. (7), λ can be interpreted as a pressure jump at the upper surface since the first term is the force on this surface connected with $g_i(h)$ and the second term is the Gibbs-Thomson pressure of a curved surface.

For a uniform film the chemical potential per particle is $\mu_{\mathrm{film}}=(1/\rho)dg_i/dh$, in agreement with the general definition $\mu\equiv\partial G/\partial N|_{p,T}=(1/L_0)\partial G/\partial n|_{p,T}$, where we have taken again the bulk free energy G_1 as zero. Here ρ is the density (particles per unit volume) and $n=h\rho$ the number of particles per unit area. It is therefore reasonable to define μ for a nonuniform film in equilibrium by

$$\mu_{\mathrm{film}}=\frac{\lambda}{\rho}=\frac{1}{\rho}\left(\frac{dg_i}{dh}-\gamma_{\mathrm{LV}}\frac{\partial^2 h}{\partial x^2}\right). \tag{8}$$

In Figs. 1, curve *a*, and 2, curve *a* we show the simplest case in which $g_i(h)$ and dg_i/dh both approach zero at $h\rightarrow\infty$, from above and below, respectively. To illustrate the manner in which the breakup of the film can occur as its thickness is reduced we consider a more complicated function $g_i(h)$ (shown in Fig. 1, curve b) in which dg_i/dh is not monotonic, as suggested by Derjaguin, Churaev, and Muller [19]. The brief description in the next paragraph summarizes the work of Sharma [9] and Mitlin [18] and emphasizes the analogy with phase separation in a two-component alloy [20,21].

We identify two phases, ''thick'' and ''thin'' films, and refer to Fig. 2, curve b, which shows $dg_i(h)/dh$. When the two phases coexist they have equal chemical potentials $\rho^{-1}dg_i(h)/dh$ and their thicknesses h_1 and h_2 are related by a Maxwell construction; a proof for the present case will be given in Sec. III B. Then (a) when $h>h_2$ or $h_1>h$ the film is stable, (b) when $h_4>h>_2$ or $h_1>h>h_3$ the film is metastable and can decompose by a nucleated transition into a two-phase arrangement of thick (h_2) and thin (h_1) layers in coexistence, and (c) when $h_3>h>h_4$ the film is unstable and spontaneously decomposes into such a two-phase arrangement, which is equivalent to spinodal decomposition in alloys. It is possible that $h_2\rightarrow\infty$, as in Fig. 3, in which case the equilibrium situation consists of macroscopically thick drops sitting on a continuous thin film. This is called autophobicity [13].

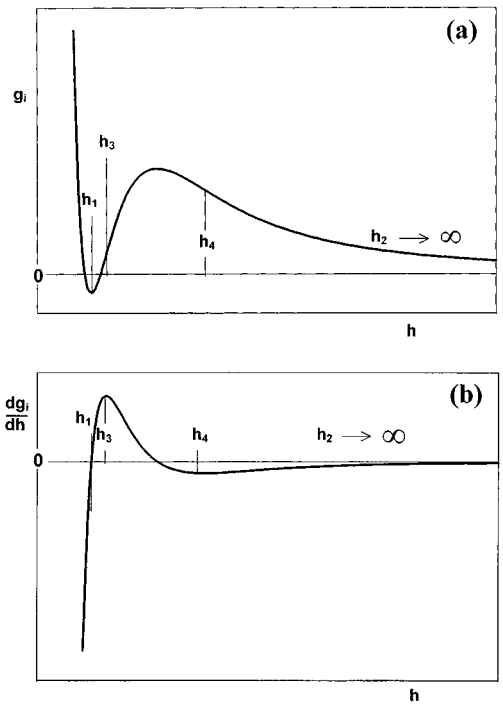

FIG. 3. (a) Interfacial Gibbs free energy g_i and (b) dg_i/dh for an autophobic system for which $h_2\rightarrow\infty$.

When we have the two thicknesses h_1 and h_2 in equilibrium, a certain transition profile $h(x)$ is created, which is the solution of Eq. (8) and represents the minimum in total energy. In the transition region $dg_i/dh-\rho\mu$ is balanced by the Gibbs-Thomson pressure

$$\frac{dg_i}{dh}-\rho\mu=\gamma_{\mathrm{LV}}\frac{\partial^2 h}{\partial x^2}, \tag{9}$$

which can be integrated from h_1 (where $\partial h/\partial x=0$) to give

$$\frac{\gamma_{\mathrm{LV}}}{2}\left(\frac{\partial h}{\partial x}\right)^2=\int_{h_1}^{h}\left(\frac{dg_i}{dh'}-\rho\mu\right)dh'$$
$$=[g_i(h)-\rho\mu h]-[g_i(h_1)-\rho\mu h_1]. \tag{10}$$

Using this relationship, we can derive an effective contact angle [11] along the edge separating the thick and thin films. It can be defined as the largest angle in the transition region and is found at the point where $g_i(h)-\rho\mu h$ is maximum. This is not a true contact angle as for a drop on a dry surface because the gradient dh/dx is actually continuous between the two regions, but in practice it looks very similar. The contact angle will be important when we discuss the pattern-formation aspects of this problem.

B. Film evolution equation

The equilibrium configuration of the film can also be obtained by writing an equation to describe its time evolution and, starting with a surface perturbation to a uniform film,

integrating until a steady state is obtained. This was done by Sharma and Jameel [10] for the one-dimensional nonvolatile case. From Eq. (8) it follows that for a film not in equilibrium the gradient of μ is

$$\frac{\partial \mu}{\partial x} = \frac{1}{\rho}\left[\frac{d}{dx}\frac{dg_i(h)}{dh} - \gamma_{\mathrm{LV}}\frac{\partial^3 h}{\partial x^3}\right]. \tag{11}$$

The length of the film is implicitly taken as constant. Assuming laminar flow with no slip at the substrate and a free upper surface, it can then be shown [10] that

$$\frac{\partial h}{\partial t} = \frac{1}{3\eta}\frac{\partial}{\partial x}\left(h^3\rho\frac{\partial \mu}{\partial x}\right) = \frac{1}{3\eta}\frac{\partial}{\partial x}\left[h^3\frac{\partial}{\partial x}\left(\frac{dg_i}{dh} - \gamma_{\mathrm{LV}}\frac{\partial^2 h}{\partial x^2}\right)\right]$$
$$= \frac{1}{3\eta}\frac{\partial}{\partial x}\left[h^3\left(\frac{\partial h}{\partial x}\frac{d^2 g_i}{dh^2} - \gamma_{\mathrm{LV}}\frac{\partial^3 h}{\partial x^3}\right)\right], \tag{12}$$

where η is the viscosity. Clearly, a stationary state is reached [cf. Eq. (7)] when

$$\frac{dg_i}{dh} - \gamma_{\mathrm{LV}}\frac{\partial^2 h}{\partial x^2} = \rho\mu = \text{const.} \tag{13}$$

III. THEORY FOR FINITE VAPOR PRESSURE

A. Thermodynamic functions of the system

We shall now assume that the film has a nonzero vapor pressure and constant extent and given density. We also assume that it is in contact with vapor of μ_{vapor} defined by the external conditions. When the vapor and film are in equilibrium, then by definition

$$\mu_{\mathrm{film}} = \mu_{\mathrm{vapor}} = \mu. \tag{14}$$

The chemical potential of the vapor is

$$\mu_{\mathrm{vapor}} = k_B T \ln(p_{\mathrm{vap}}/p_0) \tag{15}$$

and we choose the reference pressure p_0 as p_s, the pressure of saturated vapor over a thick film ($h \to \infty$). The equilibrium defined by Eq. (14) is then

$$\mu_{\mathrm{film}} = k_B T \ln(p_{\mathrm{vap}}/p_s), \tag{16}$$

where, for a uniform layer,

$$\mu_{\mathrm{film}} = \frac{\partial g}{\partial n_{p,T}} = \frac{1}{\rho}\frac{dg}{dh_{p,T}}. \tag{17}$$

Here g is the sum of the surface energy g_i and the bulk free energy, both per unit area of the film. However, the bulk free energy is zero since we have taken a thick film as our reference state. Therefore $g = g_i$.

We can now reinvestigate some of the scenarios for $g_i(h)$ described by Sharma [9], but for volatile liquids. Consider first the case of a nonpolar liquid that interacts with the substrate via Lifshitz–van der Waals (LW) interactions only (Fig. 1, curve *a*). Then $g_i(h) = -A/12\pi h^2$ in the nonretarded regime, where A is the Hamaker constant (negative for wetting). (This is called a repulsive interaction since the two interfaces repel each other to make the film thicker. We find this terminology confusing.) Thus equilibrium is obtained when

$$k_B T \ln(p/p_s) = \mu = \frac{1}{\rho}\frac{dg_i}{dh} = \frac{1}{\rho}A/6\pi h^3. \tag{18}$$

Since dg_i/dh increases monotonically to zero, Eq. (18) has only one solution for h at each value of μ and no unstable regions exist. Equilibrium thicknesses of subsaturated films of various volatile liquids on wetted substrates have been measured by Beaglehole and Christenson [16].

Now suppose that the interaction between the substrate and the film is more complicated, as shown in Fig. 1, curve b. In this example, the free energy $g_i(h)$ represents a long-range LW interaction with negative A and a shorter-range polar (double-layer) interaction of opposite sign, which has an exponential decay $\exp(-h/l_0)$. In Sharma's [9] classification this is region 4, and for consistency we use his notation

$$g_i = S^{\mathrm{LW}}\frac{d_0^2}{h^2} + S^P \exp\frac{d_0 - h}{l_0}, \tag{19}$$

where $S^{\mathrm{LW}} d_0^2 \equiv -A/12\pi$, d_0 is a molecular radius (about 0.2 nm), and l_0 is a screening distance (about 0.6 nm). Both S^{LW} and S^P have dimensions of surface energy and S^P is negative when two of the media (water and mica in this case) have polar properties. There is evidence from the experiments that the value of S^P is dependent on absorption of ions from the mica into the water, particularly in experiments at higher temperatures. In this case typical forms of $g_i(h)$ and dg_i/dh are shown in Figs. 1, curve b, and 2, curve b, respectively. If we write p_j for the vapor pressure at which $\rho k_B T \ln[p_j/p_s] = dg_i/dh|_{h_j}$ we should expect there to be stable films of the liquid in equilibrium with vapor between p_s and p_3 and below p_4, with the possibility of a two-phase region between p_3 and p_4; we shall study this region below. In the case represented by Fig. 3, stable thin films occur below p_4, but there may not be a stable thick film region, except at $p = p_s$. Experimentally, we have found that the mica-water system can demonstrate the situations shown in Figs. 1, curve b, 2, curve b, and 3.

B. Equilibrium in terms of a thermodynamic function

We can conveniently describe the behavior of the film in terms of a thermodynamic function $\Psi = g_i(n) - \mu_{\mathrm{vapor}} n$. Because it is a nonequilibrium function, defined by an external constraint (μ_{vapor}), Ψ might be called a surface availability. (It resembles the grand potential [19] of the film, $\Omega \equiv F - \mu_{\mathrm{film}} n$, but is not the same.) Then

$$\frac{d\Psi}{dn} = \frac{dg_i}{dn} - \mu_{\mathrm{vapor}} = \frac{1}{\rho}\frac{dg_i}{dh_{p,T}} - \mu_{\mathrm{vapor}}. \tag{20}$$

Since

$$\frac{dg_i}{dn_{p,T}} = \mu_{\mathrm{film}}, \tag{21}$$

Eq. (20) can be written as

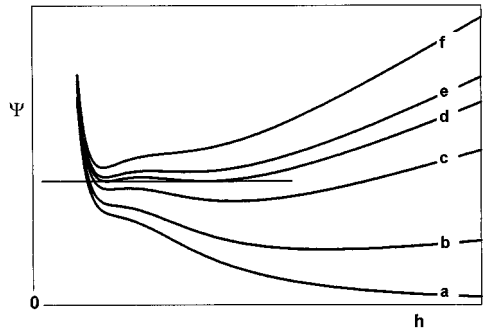

FIG. 4. Thermodynamic potential Ψ for different values of μ_{vapor}. Curve *a* represents the saturated vapor pressure at the temperature of the substrate $\mu_{\text{vapor}}=0$ [cf. Fig. 1, curve (b)], curves $b-f$ represent increasing values of $-\mu_{\text{vapor}}$, curve *d* represents phase equilibrium and curves *b* and *f* represent the situations where only the thick and thin layers, respectively, exist.

$$\frac{d\Psi}{dn}=\frac{1}{\rho}\frac{d\Psi}{dh_{p,T}}=\mu_{\text{film}}-\mu_{\text{vapor}}. \tag{22}$$

In equilibrium $\mu_{\text{film}}=\mu_{\text{vapor}}$, so we have $d\Psi/dh=0$, i.e., an extremum of $\Psi(h)$. Ψ is shown in Fig. 4, for the case of Fig. 1, curve *b* and several values of μ_{vapor} (i.e., p). There are two minima in curves c–e, which represent equilibrium thicknesses. For curve *c* (smallest $|\mu_{\text{vapor}}|$ or p closest to p_s) the minimum at large h is deepest, suggesting that the thin film is metastable and the thick film stable. For curve *e*, (largest $|\mu_{\text{vapor}}|$ of these three, i.e., lowest p) the minimum at small h is deepest, suggesting that the thin film is metastable and the thick film stable. For curve *e* (largest $|\mu_{\text{vapor}}|$ of these three, i.e., lowest p) the minimum at small h is deepest, suggesting that the thin film is stable and the thick film metastable. For curve *d* one sees the situation in which equilibrium is established between the vapor and films of both thicknesses. The two minima are now at the same height; therefore

$$0=\int_{h_1}^{h_2}d\Psi=\int_{h_1}^{h_2}\frac{d\Psi}{dh}\,dh=\int_{h_1}^{h_2}\left(\frac{dg_i}{dh}-\rho\mu_{\text{eq}}\right)dh, \tag{23}$$

which is the Maxwell construction on a diagram of dg_i/dh vs h. Here μ_{eq} is the value of $\mu_{\text{film}}=\mu_{\text{vapor}}$ for which the two thicknesses are in equilibrium. This is shown in Fig. 2, curve b. For the case shown in Fig. 3, where S^P is larger, the equilibrium value μ_{eq} is equal to zero. In this autophobic case a thin film is in equilibrium with macroscopic drops and saturated vapor. Since all this is completely analogous to the situation in any other two-phase system, we can immediately make the following statement about nonequilibrium situations, following curve *b* in Fig. 2.

When two minima exist as in Fig. 4, curves c–e, the driving force towards a global equilibrium situation in one or the other (i.e., where the whole film is either at h_1 or at h_2) is proportional to the difference in Ψ between their depths, but a transition from one to the other must be nucleated because of the barrier between them. Figure 4, curves *a*, *b*, and *f* show $\Psi(h)$ for more extreme values $\mu_{\text{vapor}}>dg_i/dh|_{h_3}$ and $\mu_{\text{vapor}}<dg_i/dh|_{h_4}$ for which only one minimum exists and no phase separation occurs.

Suppose that μ_{vapor} is reduced in small steps downward from zero. The thick film adjusts its h to each new μ_{vapor} but stays uniform until $\mu_{\text{vapor}}=\mu_{\text{eq}}$ at $h=h_2$. After that, in the absence of a nucleation event, it can continue to thin uniformly, as a metastable film, until $h=h_4$. At this point there are no longer two minima and a *non-nucleated* (spinodal) transition occurs. In fact, the nucleation barrier has been steadily falling towards zero at h_4 and a nucleated transition will always occur before that. Such nucleated transitions from $h<h_2$ and $h>h_1$ can give rise to a hysteresis effect in the dependence of h on μ_{vapor}.

If the film could be *prepared* at a thickness between h_4 and h_3, spinodal decomposition to h_1 and h_2 would occur; however, evaporation and condensation compete with the spinodal decomposition. Thus, if $\mu_{\text{vapor}}(\text{preparation})>\mu_{\text{eq}}$ the film will go via condensation to $h>h_2$, while in the opposite case it will go to $h<h_1$. Decomposition to h_1 and h_2 will only be significant if evaporation is very slow.

When a thin film is nucleated in a film thinner than h_2, a small region of the new phase is formed. The excess water does not immediately evaporate but is ejected into the surrounding film and thickens it locally. It is the ejection process and the consequent redistribution of the ejected water that cause the patterns to form.

C. Contact angles

We can now express the effective contact angle for equilibrium between the thick and the thin film through the thermodynamic potential Ψ. Equation (10) can be written

$$\frac{\gamma_{\text{LV}}}{2}\left(\frac{\partial h}{\partial x}\right)^2=[g_i(h)-\rho\mu_{\text{eq}}h]-[g_i(h_1)-\rho\mu_{\text{eq}}h_1]$$
$$=\Psi(h)-\Psi(h_1), \tag{24}$$

i.e., the largest gradient of the film occurs at the point at which $\Psi(h)$ is a maximum.

It is of interest to substitute some numbers in the formulas in order to show that the results are reasonable in comparison to experimental values. We have used the relationship (19) introduced in Sec. III A. Using this formula, there is only a very limited range of S^P for which phase separation occurs during evaporation. We shall express this in terms of the ratio $R\equiv -S^P/S^{\text{LW}}$. R has an upper bound at which autophobicity sets in at the saturated vapor pressure; i.e., the Maxwell construction gives $\mu_{\text{vapor}}=0$. It has a lower bound at which dg_i/dh becomes monotonic and therefore complete wetting occurs at all pressures. This range is given by $0.10<R<0.147$. Evaluation of $\Psi(h)$ at phase equilibrium (Fig. 4, curve *d*) then allows the contact angle to be calculated. Figure 5 shows for this range of R the results of calculations of h_1, h_2, equilibrium chemical potential μ_{eq}, and contact angle θ for the values $S^{\text{LW}}=15\ \text{mJ/m}^2$, typical for water on mica, and $\gamma_{\text{LW}}=80\ \text{mJ/m}^2$. It will be seen that the contact angle lies in the range $0<\theta<0.04$ rad, which can be compared with experimentally determined values for static contact angles in the range 0.03 ± 0.01 rad. Experimentally, h_2 is usually around 25 nm, which corresponds to $R=0.146$. However, when a freshly cleaved surface is wet repeatedly at room temperature it is possible to observe the complete range from wetting ($R<0.10$) to autophobicity ($R>0.147$), presumably because of absorption of ions, which leads to a gradual increase of $-S^P$.

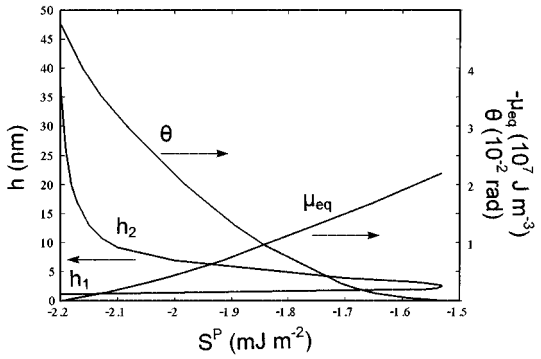

FIG. 5. Calculations of h_1, h_2, equilibrium chemical potential μ_{eq}, and contact angle θ as a function of S^P, for the values $S^{LW} = 15$ mJ/m^2 and $\gamma_{LW} = 80$ mJ/m^2, typical for water on mica.

D. Evolution of a two-dimensional film

We now continue by studying the dynamic aspects of volatile film evolution. The dynamics of nonvolatile films have already been investigated by Sharma and Jameel [10], Reiter [14], Brochard-Wyart and co-workers [15], and de Gennes [12].

Suppose that a thick film is formed and then the vapor pressure is reduced to below saturation, so that it slowly evaporates. We expect that the film will thin uniformly until the thickness is reached at which $\mu_{film} = \mu_{vapor}$. If this value is above μ_{eq} a stable uniform film remains. If μ_{vapor} is somewhat lower than μ_{eq}, the thick film stabilizes at $h < h_2$ but is now metastable and a nucleation event can cause a local phase change in which a minute patch is created where the thickness is less than or equal to h_1. We call this a dry patch. The probability of such an event increases as $h \to h_4$ because of the falling height of the nucleation barrier in Ψ (Fig. 4, curves *d* and *e*). On an isotropic substrate, the patch will initially be circular since this shape minimizes edge energy [3]. Provided its diameter is above some critical value, the patch will grow, since by doing so it reduces the total free energy of water film plus vapor, and in doing so water is ejected into its rim. Eventually enough water has been ejected for the rim height to reach thickness h_2 and local equilibrium is established around the edge; the rest of the evolution is determined by the transfer of the water from the rim into the thinner wet surrounding medium [15]. We shall show below that under some conditions this process can be described in an analogous manner to solidification from an undercooled melt and therefore expect similar instabilities to occur. In the case of a nonvolatile fluid, this evolution by hydrodynamics can be very slow. In our case, since the film is evaporating the process is accelerated by transport through the vapor phase, which prevents the equilibrium height h_2 being achieved at the rim.

We shall now formulate this part of the process mathematically. The field variable is $h(x,y)$. The h-dependent part of the free energy of the film is, by analogy with Eq. (2),

$$G = \int\int g_i(h(x,y)) = \frac{\gamma_{LV}}{2} |\nabla h|^2 dx\, dy. \tag{25}$$

The volume of the film is h per unit area so that the total volume is

$$\int\int h(x,y) dx\, dy. \tag{26}$$

Consider the two-dimensional analog to Eq. (12):

$$\left.\frac{\partial h}{\partial t}\right|_{flow} = \nabla \cdot \frac{h^3}{3\eta} \nabla \left[\frac{dg_i(h)}{dh} - \gamma \nabla^2 h \right]. \tag{27}$$

We add to this a term that represents the evaporation. The rate of evaporation depends linearly on the difference between the chemical potential of the vapor and that of the film, with a constant of proportionality α that is a temperature-dependent parameter whose value can be estimated from kinetic theory of gases or determined experimentally. Then we have, from Eq. (27),

$$\left.\frac{\partial h}{\partial t}\right|_{total} = \nabla \cdot \frac{h^3}{3\eta} \nabla \left[\frac{dg_i(h)}{dh} - \gamma \nabla^2 h \right] - \frac{\alpha}{\rho} \left[\frac{dg_i(h)}{dh} - \gamma \nabla^2 h - \rho \mu_{vapor} \right]. \tag{28}$$

This equation contains both second-order and higher differentials. When the second-order terms dominate, it has the form of a diffusion equation, and on this is based the analogy with diffusion-controlled growth. When the higher-order terms dominate, the evolution is comparable to that in hydrodynamic systems (e.g., viscous fingering). To emphasize this formulation [22] we shall linearize Eq. (28) about the thick equilibrium film by writing $\delta h \equiv (h - h_2)$ and concentrate our attention on the thick region (i.e., outside the rim of the patch). In the linear approximation $dg_i/dh = dg_i/dh|_{h_2} + d^2 g_i/dh^2|_{h_2} \delta h$. Then Eq. (28) becomes

$$\frac{\partial \delta h}{\partial t} = \frac{h_2^3}{3\eta} \left[\left.\frac{d^2 g_i}{dh^2}\right|_{h_2} \nabla^2 \delta h - \gamma \nabla^4 \delta h \right] - \frac{\alpha}{\rho} \left[\left.\frac{dg_i}{dh}\right|_{h_2} - \rho \mu_{vapor} - \gamma \nabla^2 \delta h \right]. \tag{29}$$

This equation contains three types of terms: (a) a linear term proportional to $dg_i/dh|_{h_2} - \mu_{vapor}$, which leads to evaporation or condensation depending on the deviation of the mean thickness from equilibrium with the vapor; (b) second-order spatial differentials of the profile, leading to an effective diffusion coefficient $D_{eff} = d^2 g_i/dh^2|_{h_2} h_2^3/3\eta + \alpha\gamma/\rho$ [the latter term (D_e) is always positive and the former (D_s) is also positive outside the spinodal region]; and (c) fourth-order spatial differentials, giving hydrodynamic effects.

To appreciate the relative importance of the second- and fourth-order differential terms we must estimate typical orders of magnitude. It is interesting that for the model substrate interaction discussed above and using a value for α derived from our experiments. The two contributions to the effective diffusion constant are found to be similar in magnitude. It is difficult to estimate α from kinetic theory because the calculation involves a ''sticking coefficient,'' whose value is not well established, for vapor molecules hitting the water surface.

Typically, for the parameters used in the estimates of Sec. III C (with $S^P=-2.15$ mJ/m^2 and $\eta=0.001$ kg/m s), we find $dg_i/dh|_{h_2}\sim-6\times10^2$ J/m^3 and $d^2g_i/dh^2|_{h_2}\sim2\times10^{11}$ J/m^4. From these values one can estimate the two contributions to the effective diffusion constant as $D_s\sim10^{-10}$ m^2/s for the substrate interaction term and $D_e<8\times10^{-9}$ m^2/s for the evaporation term (depending on the value of the sticking coefficient).

A comparison between the ''diffusionlike'' and hydrodynamic terms can only be made at a given length scale. For example, if we choose to look at height structures on the scale (in x-y) of $\lambda=10$ μm, for which we can write $\nabla\equiv ik\sim2\pi i/\lambda$, we have, in the linear limit ($\delta h\to0$),

$$\frac{\partial\delta h}{\partial t}\approx-Dk^2\delta h-\frac{\gamma h_2^3}{3\eta}k^4\delta h. \tag{30}$$

For the given value of k, the first term is about $100\delta h$ and the second about δh, so that it is reasonable as a first approximation to consider the diffusion approximation only, although for thicker films the hydrodynamic term becomes important since the second term is proportional to h_2^3.

E. Analogy with diffusion-controlled growth models

One purpose of this paper is to establish an analogy between the evolution of the film as it evaporates and existing growth models. Under the conditions where the second-order differentials dominate there is a rather complete analogy with the models developed for growth of a solid from its melt in two dimensions [1,2]. However, the correspondence to the solid-liquid problem is not straightforward because the surface profile is continuous between adjoining thin and thick films. With this reservation, the expanding dry patch corresponds to the solid and the thick film to the liquid phase. During the expansion, water is ejected into the surrounding medium at a rate of $(h_2-h_1)v$, where v is the normal velocity of the interface between the two regions, and local equilibrium is established at the interface. Thus h_2-h_1 corresponds to the latent heat in the solidification model. Growth of the patch continues because the surrounding thick film, which evaporates continuously, has thickness $h(x,y)$ less than h_2 so that water diffuses into it following Eq. (29). The boundary conditions driving this diffusion are the rim of the dry patch ($h\cong h_2$) and the conditions at infinity (the rim being the source and infinity the sink), where the dimensionless supersaturation $\Delta=[\mu_{\rm eq}-\mu_{\rm film}(\infty)]/\mu_{\rm eq}$, by analogy with the expression appearing in the solidification problem. This Δ is the parameter that we can control by the evaporation rate through the vapor pressure above the film.

When the interface is curved the supersaturation at the interface is modified by the Gibbs-Thomson curvature correction, which in the solidification models [2] gives interface supersaturation $\Delta-d_0K$, where d_0 is the capillary length and K is the interface curvature. It is of interest to establish the equivalent to d_0 in the present situation since it is an important parameter in growth models and the critical nucleus for growth has radius d_0/Δ [21].

In one dimension we had [Eq. (13)] $dg_i/dh-\gamma h_{xx}=\rho\mu_{\rm film}$ in equilibrium. Now we have $dg_i/dh(x,y)-\gamma(h_{xx}+h_{yy})=\rho\mu_{\rm film}$. Consider the configuration of a circular patch of thickness h_1 and radius R, where R is the position of largest h_r. For axial symmetry we write

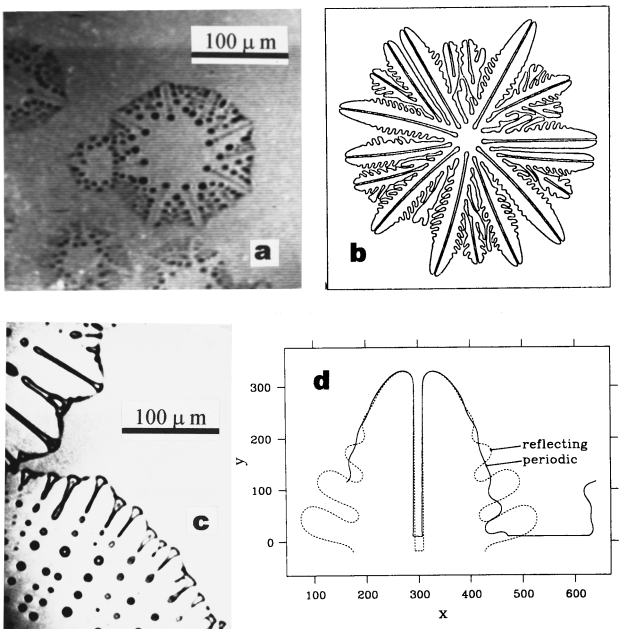

FIG. 6. Comparison of water film evaporation patterns at large subsaturation with simulations of two-dimensional crystal growth under similar conditions. (a) Fully developed pattern around a dry patch at $\Delta=0.9$ [3], (b) simulation of two-dimensional isotropic solid growth at $\Delta=0.7$ [5], (c) meeting of two drying fronts moving into a wet region at $\Delta=0.9$ [8], and (d) isotropic growth simulation showing the doublon structure at $\Delta=0.7$ [6].

$$\frac{dg_i}{dh}(r)-\gamma(h_{rr}+h_r/r)=\rho\mu_{\rm film}, \tag{31}$$

which can be written

$$\frac{dg_i}{dh}(r)-\gamma h_{rr}=\rho\mu_{\rm film}+\gamma h_r/r=\left.\frac{dg_i}{dh}\right|_{h_2}+\gamma h_r/r. \tag{32}$$

So it follows that $dg_i/dh|_{h_2}+\gamma h_r/r$ replaces $dg_i/dh|_{h_2}$ when the interface is curved. On the edge $h_r|_R\leqslant\theta$ (contact angle). For estimation, we replace $\leqslant$ by $=$ and then have at R the boundary condition for $dg_i/dh-\gamma h_{rr}$ that $\mu(R)=\mu_{\rm eq}+\gamma\theta K/\rho$, where $K=1/R$. Thus $d_0=\gamma\theta/\rho|\mu_{\rm film}|$. This expression has a value, for the typical conditions quoted above, of about 4 μm. Since Δ is of order unity in our experiments, this value agrees with observations of the dimensions of nucleated patches. We could also calculate an effective diffusion constant in the dry phase, but this is generally not included in the solidification models since the solid phase has uniform temperature and does not evolve.

Indeed, the form of the instability observed in these experiments corresponds in some respects very well with typical features of solidification simulations [6,5]. We point out in particular the formation of features called doublons or parity-broken dendrites, which appear in the simulations of isotropic materials in two dimensions at large supercooling Δ and therefore have rarely been observed in crystal growth

experiments. Two examples of comparable features are shown in Fig. 6, but further quantitative details will be presented elsewhere [8].

F. Hydrodynamic instability region

When the amplitude of the instability grows, eventually the thick film realizes conditions where the approximation we made by neglecting the fourth-order term in Eq. (29) becomes invalid. For thick enough films we can neglect the second-order term instead and obtain

$$\frac{\partial h}{\partial t} = -\nabla \cdot \frac{h^3}{3\eta} \nabla [\gamma \nabla^2 h] \tag{33}$$

for the late-stage evolution of the film. This problem, which leads to a Rayleigh-type instability and eventually to formation of a periodic array of drops, has already been discussed in elementary form [7] and can also be seen in the experimental examples of Fig. 6. The evolution occurs in the presence of a fixed contact angle along the boundary. The quantitative comparison between this instability and the experiments will also be discussed in detail elsewhere [8]. Neither the full development in the hydrodynamic regime nor that in the intermediate region, where the two terms on the right-hand side of Eq. (27) have comparable magnitude, has yet been treated, but we encourage computer simulations of the problem in the future.

ACKNOWLEDGMENTS

This work has evolved from the initial experiments carried out by M. Elbaum and the critique of R. Kupferman, through illuminating discussions with A. Oron, H. Müller-Krumbhaar, and E. Brener, and correspondence with A. Sharma and J. Cahn. The research was supported by the German-Israeli Binational Science Foundation, the Minerva Center for Non-linear Science, and the Technion Fund for the Promotion of Research.

[1] Eshel Ben-Jacob, Contemp. Phys. **34**, 247 (1993).
[2] J. S. Langer, Science **243**, 1150 (1989); J. S. Langer, in *Chance and Matter*, Proceedings of the Les Houches Summer School of Theoretical Physics, Les Houches, 1986, edited by J. Souletie, J. Vannimenus, and R. Stora (North-Holland, Amsterdam, 1987).
[3] M. Elbaum and S. G. Lipson, Phys. Rev. Lett. **72**, 3562 (1994).
[4] M. Elbaum and S. G. Lipson, Isr. J. Chem. **35**, 27 (1995).
[5] R. Kupferman, O. Shochet, and E. Ben-Jacob, Phys. Rev. E **50**, 1005 (1994).
[6] T. Ihle and H. Müller-Krumbhaar, Phys. Rev. Lett. **70**, 3083 (1993); Phys. Rev. E **49**, 2972 (1994).
[7] S. G. Lipson, Phys. Scr. **T67**, 63 (1996).
[8] N. Samid-Merzel, S. G. Lipson, and D. S. Tannhauser (unpublished).
[9] A. Sharma, Langmuir **9**, 861 (1993).
[10] A. Sharma and A. T. Jameel, J. Colloid Interface Sci. **161**, 190 (1993).
[11] A. T. Jameel and A. Sharma, J. Colloid Interface Sci. **164**, 416 (1994).
[12] P. G. de Gennes, Rev. Mod. Phys. **57**, 827 (1995).
[13] Jacob Israelachvili, *Intermolecular and Surface Forces*, 2nd ed. (Academic, London, 1991).
[14] G. Reiter, Phys. Rev. Lett. **68**, 75 (1992); Langmuir **9**, 1344 (1993).
[15] F. Brochard-Wyart and J. Daillant, Can. J. Phys. **68**, 1084 (1990); C. Redon, F. Brochard-Wyart, and F. Rondelez, Phys. Rev. Lett. **66**, 715 (1991).
[16] D. Beaglehole and H. K. Christenson, J. Phys. Chem. **96**, 3395 (1992).
[17] M. Elbaum, S. G. Lipson, and J. S. Wettlaufer, Europhys. Lett. **29**, 457 (1995).
[18] V. S. Mitlin, J. Colloid Interface Sci. **156**, 491 (1993).
[19] B. V. Derjaguin, N. V. Churaev, and V. M. Muller, *Surface Forces* (Consultants Bureau, New York, 1987); L. D. Landau and E. M. Lifshitz, *Statistical Physics*, 2nd ed. (Pergamon, Oxford, 1980).
[20] J. W. Cahn, Trans. Metall. Soc. AIME **242**, 166 (1968).
[21] D. A. Porter and K. E. Easterling, *Phase Transformations in Metals and Alloys*, 2nd ed. (Van Nostrand Reinhold, New York, 1992).
[22] E. Brener and H. Müller-Krumbhaar (private communication).